Journal of GeoEngineering, Vol. 12, No. 2, pp. 81-88, June 2017
http://dx.doi.org/10.6310/jog.2017.12(2).4

EXCAVATION WITHOUT INTERNAL SUPPORT AND ITS IMPLICATIONS IN CONSTRUCTION MANAGEMENT：A CASE STUDY

Pei-Yan Lin [1*], Teng-Kuei Chang [2], Shu-Ken Ho [3], and S. Ping Ho [4]

ABSTRACT

This paper presents a case study of a basement construction during building renovation, where an underground tube-like retaining structure was constructed with a strut-free support system. This underground structure was formed by combining a new arch diaphragm wall built outside the old basement and an arch reinforced concrete wall constructed inside the old basement. The arch reinforced concrete wall was connected to the old substructure or basement. Pile installation, excavation, and demolition were conducted inside this tube-like retaining structure. The lateral displacement of the retaining wall and soil and the stress of the rebar in the diaphragm wall and the ground settlement surrounding the construction site were measured at each stage of the construction. Field measurements indicate that after the completion of the new substructure, the maximum displacement of the wall was 20 mm, which was about 0.1% of the final excavation depth. These values were much smaller than the values obtained in the common excavations in Taipei. The field measurement results demonstrate that the combination of a new arch diaphragm wall and an old retaining wall support system is feasible in a building renovation context. This method reduces not only the construction cost but also the construction duration by up to 6 months.

Key words: Building renovation, tube-like retaining structure, strut-free support, seismic isolation system.

1. INTRODUCTION

Construction of a building foundation normally involves four activities: The installation of an earth retention structure, followed by excavation and strut installation, and finally construction of the foundation. Many case studies have proven that a well-installed earth retention structure is beneficial in reducing the strutting work, and thus the cost of construction and construction time; it also improves the feasibility of construction. For instance, adopting a tube-like retaining structure to develop the transversal arch effect can counteract some or all of the lateral earth pressure. As studied by Ou *et al*. (1996), with the arching effect of the retaining wall, the wall deflection can be reduced to a small amount. Use of this approach may involve a lesser support system, or even no support system.

Tube-like structures are known for their self-developed arch effects, replacing the need for struts during excavation. Construction of underground gas storage tanks or tunnel shafts is typical examples. Suroor *et al*. (2008) presented two similar gas storage tank basins with diameter of 18.29 m and depth of 9.8 m and the excavation was retained by concrete secant pile walls without support. Tan *et al*. (2013) described a large diameters cylindrical self-supported excavation of 100 m diameter and 25.89 m deep in Shanghai soft clay. Lee *et al*. (2005) have presented an excavation case study with a strut-free support system by using a 140 m-diameter circular diaphragm wall for the Kaohsiung Mass Rapid Transit System.

This paper presents a building renovation project located at the heart of Taipei for an existing four-level basement. The new facade of the building renovation is displayed in Fig. 1(a). The new building has spiral-like upper floors with extending spans that were not supported by columns directly, as shown in Fig. 1(b). The building's structure is composed of a cylindrical core tower with two wing towers on opposing sides. Since the superstructure projected on the ground is circular, the new basement was designed to also have a circular shape. In order to enhance the anti-seismic ability, a seismic isolation system was installed on the foundation slab. Hence, the self-standing retaining wall shaped as a tube-like structure was adopted. Use of the tube-like retention structure ensures safety during excavation and saves on project costs.

2. PROJECT BACKGROUND

The old building, built in 1997, consisted of 14 stories above the ground level and 4 basement levels. The old hexagonal basement was 18 m in depth below the ground level. Pile foundations were used as the foundation system. An open-roofed atrium from B3 to the ground floor was located in the center of the old building. The old diaphragm wall had a thickness of 1 m and a depth of 36 m and was also used as the exterior wall of the basement. Figure 2 shows the old building layout.

The renewal was designed with 21 stories above the ground level and 4 basement levels. The depth of the new basement remains the same. The new foundation slab is located directly on the old foundation slab. To meet the safety requirements, a seismic isolation system was installed for the newly designed cylindrical basement, in which the self-standing retaining wall was adopted as a permanent tube-like structure with an inner diameter of 74 m.

Manuscript received December 6, 2016; revised January 26, 2017; accepted February 7, 2017.

[1] Ph.D. Candidate (corresponding author), Department of Civil Engineering, National Taiwan University, Taipei, Taiwan (e-mail: pylin56912@yahoo.com.tw).
[2] Technical Manager, Sino Geotechnology, Inc., Taipei, Taiwan.
[3] Chief Engineer, Sino Geotechnology, Inc., Taipei, Taiwan.
[4] Professor, Department of Civil Engineering, National Taiwan University, Taipei, Taiwan.

(a)

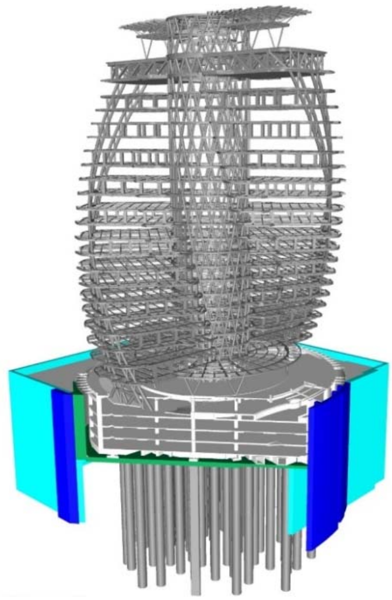

(b)

Fig. 1 (a) Appearance of new building; (b) Structure model of new building

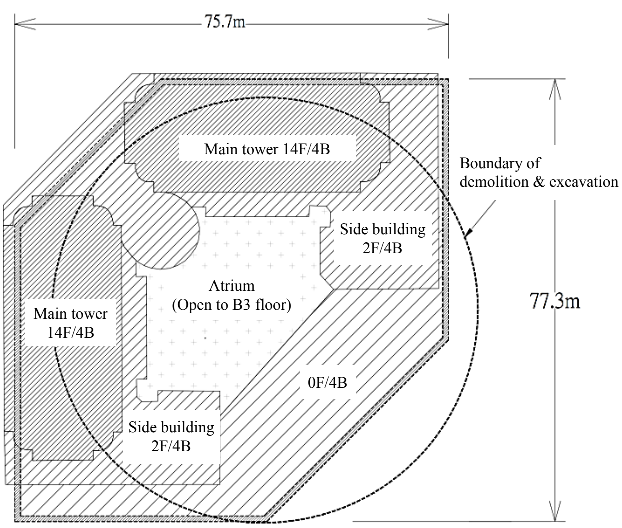

Fig. 2 Layout plan of the old building

Since the new basement area exceeded the range of the old one, a new arch diaphragm wall (see ABCDE in Fig. 3), having a thickness of 1.0 m and 1.5 m and depth of 36 m, was built outside the old basement area. Buttresses of 1.0 m thickness and 1.5 m length were constructed to connect the new arch diaphragm wall at every 4.8 m interval. Another 60-cm-thick reinforced concrete (RC) wall, FGH as shown in Fig. 3, was constructed in the old basement area. This RC wall was connected to the old substructure frame and the old diaphragm wall to form an integrated retaining structure system. The RC wall and the new arch diaphragm wall formed a tube-like retaining structure.

After completion of the tube-like structure, excavation and demolition were conducted in the area of the new basement. Then, the new foundation slab was cast and the self-standing retaining wall was used as a permanent retaining structure, as shown in Fig. 4.

A pile foundation was used in this new building. The old piles in the original buildings were kept as part of the foundation. The new piles, 2 m in diameter, were installed and penetrated into bedrock approximately 1.5 to 2.5 m deep, such that the bottom of pile was about 47.5 m to 53.5 m below the ground level. There were 52 old piles with a diameter of 1.5 m and located 36 m deep below the ground level. Figure 5 shows the arrangement of the piles.

Although the retaining wall is circular in shape, the structural stiffness is not symmetrical because the tube-like retaining wall was with different thickness or stiffness in some sections. A foreseeable unsymmetrical deformation of the retaining wall during construction had to be considered. Therefore, a comprehensive monitoring system was installed to observe the displacement of the retaining wall at each construction phase to ensure the quality and safety of the entire construction process.

The monitoring system, whose layout is shown in Fig. 6, was mainly used to observe the lateral displacements of the soil and the retaining wall, and the ground settlement caused by the new basement construction. All inclinometers, except SID-4 and

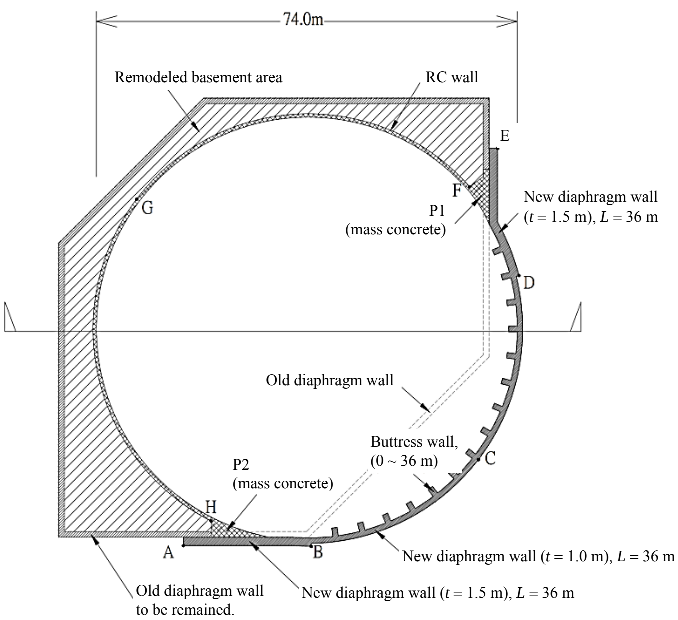

Fig. 3 Layout plan of the new self-standing retaining structure system

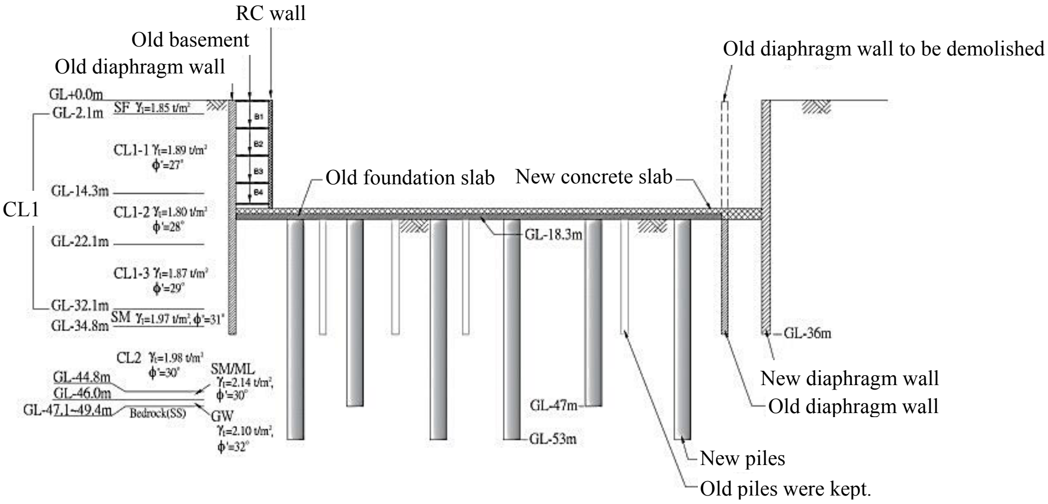

Fig. 4 Profile of the new self-standing retaining structure system

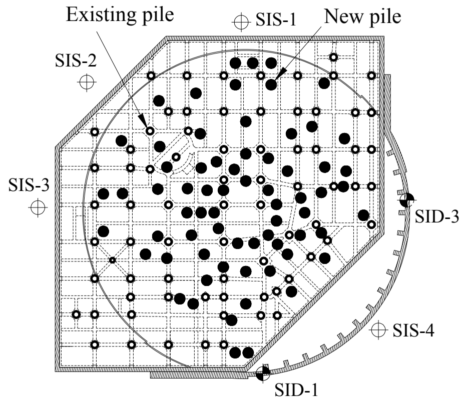

Fig. 5 Layout plan of the old and new piles

SID-5, were installed into soil layer 7 (GW) at least 3 m as fixed reference points. The inclinometers SID-1 and SID-3 were embedded in the new arch diaphragm wall and were extended to the gravel layer. SIS-4 was installed in the soil outside of the new arch diaphragm wall after the completion of phase I to replace the failed SID-2. Thus, SIS-4 was only used to observe the soil lateral displacement during construction phase II (pile construction phase) and phase III (excavation and demolition in the tube-like structure). SID-4 and SID-5 were installed in the arch RC wall and its bottom was located at the depth of the foundation slab to observe the displacement of the RC wall during construction phase III. SIS-1, SIS-2, and SIS-3 were installed in the soil outside the old basement after the completion of the new diaphragm wall and their bottom was also keyed into the gravel layer by 3 m.

The rebar strain gauges at the various depths at the location of RS-1, RS-2, and RS-3 were installed on the horizontal and vertical rebar, as shown in Fig. 6. RS-1 and RS-3 were placed on the connection between the old and new retaining structures, where stress conditions are complicated.

The settlement gauges for monitoring the ground surface settlement were also shown in Fig. 6. Because of the constraint of the surrounding environment, the gauges were randomly distributed around the reconstruction site.

3. GROUND CONDITIONS

This project site is located on the fringe of the south-east Taipei Basin. The Taipei Basin mainly comprises sediment of Quaternary and Holocene alluvium, a deposit of clay, sand, and gravel, under which the Tertiary bedrock lies (Woo 1990). Investigation of the ground composition was carried out 65 m below the surface. The subsurface soil profile can be divided into 7 sub-layers, as shown in Fig. 4. Typical soil physical and strength properties are presented in Table 1 and the soil characteristics are described as follows:

(1) Backfill (SF):

This layer occupies the space between the ground surface and 2.5 m below the ground surface. The average thickness of this layer is 2.1 m. Its components are yellowish-brown silty sand with gravel and brick fragments.

(2) Silty clay (CL1):

The main content of this layer is gray silty clay occasionally containing shell fragments and/or decayed wood. This layer is found between approximately 2.0 m and 33.1 m below the ground surface. The average thickness of this layer is 30 m. Based on the Standard Penetration Test (STP)-*N* value, this layer can be divided into three sublayers as below:

Upper layer (CL1-1)

This sub-layer is found between 2.0 m and 16.4 m below the ground surface with an average thickness of about 12.2 m. The *N* value ranges from 1 to 3 and the average *N* value is about 2, indicating that the soil is very soft to soft in consistency.

Middle layer (CL1-2)

This sub-layer is found between 12.6 m and 23 m below the ground surface with an average thickness of about 7.8 m. The *N* value ranges from 3 to 4 and the average *N* value is about 3.5, indicating that the soil is soft in consistency.

Lower layer (CL1-3)

This sub-layer is found between 20.2 m and 33.3 m below the ground surface with an average thickness of about 10.0 m. The *N* value ranged from 5 to 8 and the average *N* value is about 5.5, indicating that the soil is medium stiff to stiff in consistency.

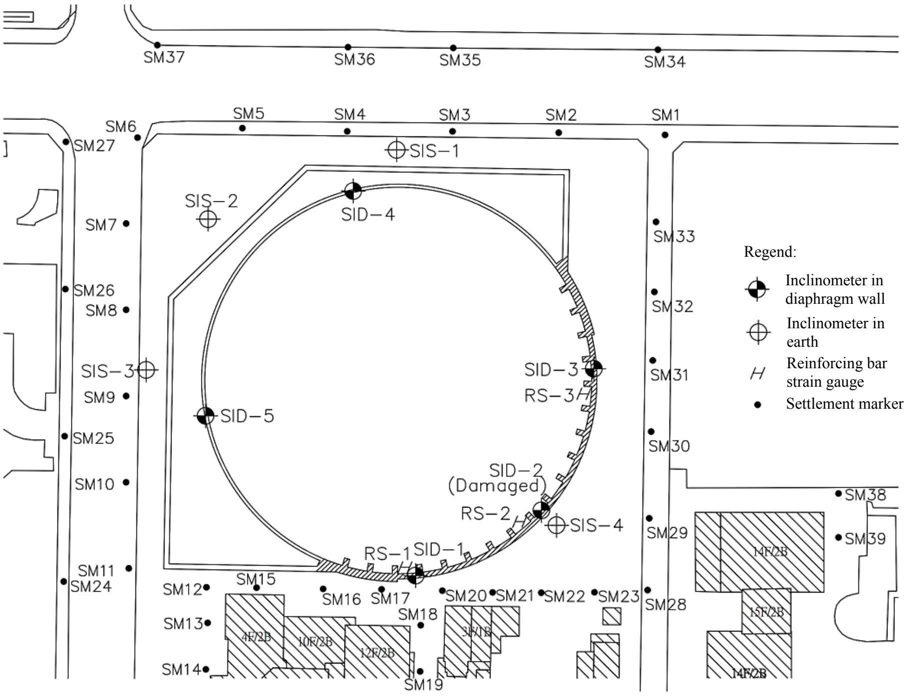

Fig. 6 Layout plan of the monitoring system

Table 1 Soil properties of the site

No.	Soil type		Depth (m)	SPT-N (average)	γ_t (kN/m^3)	ω_n (%)	ω_L (%)	I_p (%)	c (kPa)	ϕ (kPa)	s_u (kPa)
1	Backfill (SF)		0.0 ~ 2.5	~	18.5	~	~		0	28	~
2	Silty clay (CL1)	(a) Upper layer	2.0 ~ 16.4	1 ~ 3(2)	18.9	35	35	13	0	27	20 ~ 40
		(b) Middle layer	12.6 ~ 23	2 ~ 5(3.5)	18.0	42	48	24	0	28	40 ~ 60
		(c) Lower layer	20.2 ~ 33.3	4 ~ 9(5.5)	18.7	36	40	17	0	29	60 ~ 80
3	Silty sand (SM)		29.9 ~ 38	10 ~ 37(19)	19.7	23	~	~	0	31	~
4	Silty clay (CL2)		30.8 ~ 47.8	7 ~ 29(15)	19.8	28	36	17	0	30	80 ~ 120
5	Silty sand / sandy silt (SM/ML)		44 ~ 46	13 ~ 28(21)	21.4	19	~	~	0	32	~
6	Gravelly cobbles (GW)		43 ~ 49.4	> 50	21.0	~	~	~	0	40	~
7	Bedrock (SS)		> 47.1	> 50	24.0	~	~	~	~	~	~

ω_n: Natural water content
ω_L: Liquid limit

(3) Silty sand (SM):

This layer is distributed between 29.9 m and 38 m below the ground surface. The average thickness is 2.7 m. The major content of this layer is gray silty fine sand occasionally containing gravel and weathered rock. The *N* value ranges from 10 to 37 and the average *N* value is about 19, indicating that the soil is medium dense to dense in consistency.

(4) Silty clay (CL2):

This layer is distributed between 30.8 m and 47.8 m below the ground surface. The average thickness is 10 m. The main content of this layer is gray to yellowish-brown silty clay, occasionally containing sand seams and shell fragments. The *N* value ranges from 7 to 29, with the majority of values falling between 9 and 15, and the average value at about 15, indicating that the soil is medium stiff to stiff in consistency.

(5) Silty sand and sandy silt (SM/ML):

This layer is distributed between 44 m and 46 m below the ground surface. The main content of this layer is gray silty clay with coarse to fine sand and sandy silt, occasionally containing some weathered rock. The *N* value ranges from 13 to 28 and the average is about 21, which indicates that the soil is medium dense in consistency.

(6) Gravelly cobbles (GW):

This layer is distributed between 43 m and 49 m below the ground surface with depth increasing in the south-west direction. The major content of this layer is gray cobble with coarse to fine sand. The *N* values are all greater than 50, which indicates a very dense soil consistency.

(7) Bedrock (SS):

The bedrock is primarily composed of yellowish brown to gray sandstone and siltstone, occasionally with thinly bedded shale and is encountered at around 47.1 ~ 49.4 m below the ground surface, to the depths of the borehole drilled. The *N* values are all greater than 50.

The ground water level at the construction site was 2.5 m to 5.1 m below the ground surface. The water level in the layer of silty sand (SM) at 33 m to 38 m below the ground surface was measured and found to be between 11.4 m to 12.1 m below the ground surface, which had a pressure less than the hydrostatic water pressure by 90 to 100 kPa.

4. CONSTRUCTION PROCEDURE

The tube-like retaining structure for building renovation of the basement proceeded in compliance with the planned three construction phases. Figure 7 shows the scope of work for each construction phase. In each phase, several working activities were to be carried out. Table 2 shows the schedule of the working activities in each construction phase.

In Phase I, a tube-like structure, which was also used as a permanent external wall of the basement, was built. At first, a new arch diaphragm wall, ABCDE as shown in Fig. 3, was built outside the old basement area (activity I-1). Second, the area E1 of the old building basement (see Fig. 7) was demolished (activity I-2). Then, an RC wall was built (see FGH in Fig. 3) and connected to the old substructure (see Fig. 4) inside of the old basement area (activity I-3). Finally, the old diaphragm wall was demolished (see LM and IJ in Fig. 7) from the bottom of the basement to the ground level step by step, each step being about 2 m (activity I-4). The mass concrete, as shown by P1 and P2 in Fig. 3, was constructed following each step of demolition of the old diaphragm wall up to the ground level. After finishing all the steps of demolition and construction, a new tube-like retaining structure was formed.

In Phase II, 68 new piles were installed (see Fig. 5). Since the old building basement in the area E1 had been demolished, a steel deck was constructed and connected to the first floor slab. The deck was used as a working platform in the E1 area (activity II-1) for piling (activity II-2).

Phase III included the excavation in area A1 (activity III-1), the demolition of the old basement in area E2 (activity III-2), and the demolition of a part of the old diaphragm wall, as shown by JKL in Fig. 7 (activity III-3). Subsequently, the new foundation slab was cast (activity III-4), which was the last activity to complete the tube-like retaining structure for the renewal basement. Figure 8 shows the photo of the new tube-like retaining wall.

5. MONITORING RESULTS AND DISCUSSION

5.1 Lateral Displacement

<u>Phase I Constructing the Tube-Like Retaining Structure:</u>

The lateral displacements of the diaphragm wall at SID-1 and SID-3 after completion of phase I construction are shown in Fig. 9(a). The displacement measurement was taken on 2014/3/25 with the initial readings taken on 2013/7/31, which was prior to activity I-2. As shown in the figure, the diaphragm wall deformed as a cantilever and the maximum wall displacements at SID-1 and SID-3 were 4 mm and 8 mm, respectively.

The lateral displacements of the soil at SIS-1, SIS-2, and SIS-3 after completion of phase I construction are shown in Fig. 10(a). The measurements were taken on exactly the same dates as for those of SID-1 and SID-3. As shown in the figure, the maximum wall displacements at SIS-1, SIS-2, and SIS-3 were 8 mm, 1 mm, and 6 mm, respectively, and they deformed as a cantilever.

Table 2 Schedule of working activities

Phase	Activity	Date	Summary	Activities
I	I-1	2013/01/28 to 2013/04/23	Construction of the tube-like retaining structure	New diaphragm wall, ABCDE, construction: An arch diaphragm wall, 36 m in depth, 80 m in arc length, spanning 125 radians, and 1 m (BCD) and 1.5 m (AB, DE) in thickness was built outside of the old basement area.
	I-2	2013/09/01 to 2013/11/30		Area E1 demolition: The task of demolishing the old basement in area E1 was to provide a feasible working space for hoisting operations during construction. A thorough inspection for the remaining substructure (E2) was completed to secure the structural stability after E1 demolition.
	I-3	2013/09/01 to 2014/01/10		New RC wall, FGH, construction: An arch RC wall, 60 cm in thickness, 200 m in arc length spanning 235 radians, connected to existing (old) substructure was built in the old basement area.
	I-4	2013/11/30 to 2014/03/20		Closure of activity I-1 and I-3: Demolition of the old diaphragm wall IJ and LM about 2 m at a time, step by step from the basement bottom to the ground level. After each demolition step of diaphragm wall, mass concrete (P1, P2) was used to finish the new diaphragm wall (activity I-1) and the new RC wall (activity I-3)
II	II-1	2013/12/13 to 2014/01/29	Pile installation.	Working platform: A working platform for pile installation was installed.
	II-2	2014/02/21 to 2014/05/26		Pile drilling work: 68 pieces of 2-m-diameter piles with sleeves were driven from the old foundation slab into bedrock.
III	III-1	2014/06/01 to 2014/07/10	Excavation, demolition, and construction of the new foundation slab.	A1 excavation: After the circular retaining structure was completed, arching effect developed and applied to the excavation of area A1.
	III-2	2014/06/01 to 2014/09/30		E2 Demolition: Demolition of the rest of old basement in the E2 area was completed.
	III-3	2014/06/01 to 2014/09/27		Demolition of old diaphragm wall: At the same time of A1 excavation, demolition of the old remaining diaphragm wall JKL inside the new basement area from the old foundation slab to the ground surface was completed.
	III-4	2014/09/02 to 2014/12/23		New foundation slab: The new foundation slab at a depth of 18 m was cast subsequently.

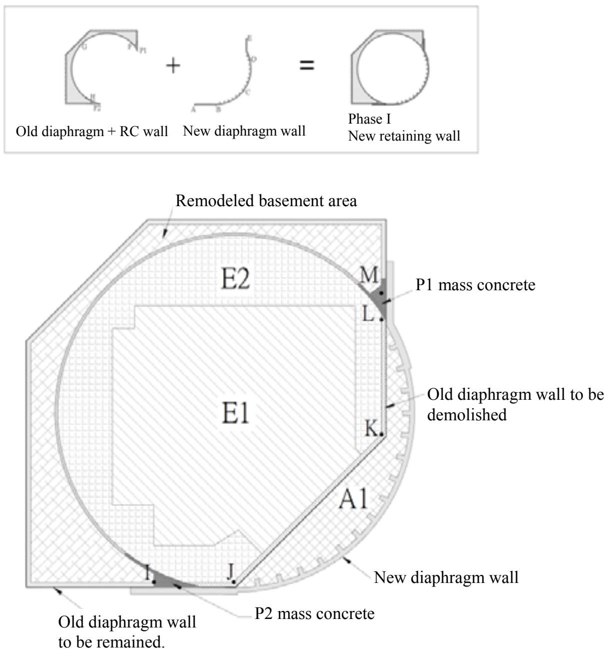

Fig. 7 The scope of work for construction phases

Fig. 8 Photo of the new tube-like retaining wall structure

The maximum deformation at SIS-2 was found to be inconsistent with that at other inclinometers. It may be due to the fact that SIS-2 was located farthest from P1 and P2, which were points of structural weaknesses during the removal of the old diaphragm wall and the old substructure prior to the closure of RC wall and new diaphragm wall (activity I-4). The displacement below the depth of 18 m at SIS-1, SIS-2, and SIS-3 was relatively small and increased abruptly above the depth of 18 m. These displacements can be assumed to be from the effect caused by restraint of the old foundation slab. Conversely, no such behavior was observed at SID-1 and SID-3, whose depths and positions did not directly connect to the old foundation slab.

Phase II Pile Installation:

The lateral displacements of the diaphragm wall at SID-1, SIS-4, and SID-3 after the completion of phase II construction are shown in Fig. 9(b). The displacement measurements were taken on 26/5/2014 with the initial readings set on 25/3/2014, at the early stage of pile installation. As shown in the figure, the maximum positive displacements of the diaphragm wall at SID-1, SIS-4, and SID-3 were 10 mm, 1 mm, and 1 mm, respectively. Negative displacements of −9 mm, −3 mm, and −4 mm, respectively, were also found at the top.

The lateral displacement of the soil at SIS-1, SIS-2, and SIS-3 after the completion of phase II construction are shown in Fig. 10(b). The measurements were taken on exactly the same dates as for those of SID-1, SIS-4, and SID-3. As shown in the figure, the maximum positive displacements at SIS-1, SIS-2, and SIS-3 were 5 mm, 2 mm, and 0 mm, respectively. Negative displacements of −3 mm, −4 mm, and −1 mm, respectively, were also found at the top.

The data of SIS-1 and SID-1 indicated a large inward displacement beneath the foundation slab during the construction phase II. This occurrence was apparently caused by piling work. A maximum displacement of 10 mm was found at SID-1 and about 5 mm at SIS-1. Since SIS-1 and SID-1 were all close to newly installed piles (Fig. 5), it is assumed that the soil removal during piling work caused an inward lateral earth displacement. While SID-1 was near two newly installed piles with the closest distance being 2.6 m, the inclinometer of SIS-1 was near five newly installed piles with a closest distance of 10 m. The distance to the pile was more influential than the number of nearby piles for the lateral displacement of inclinometers. When the section of the inclinometers at the deeper level moved inward, the top of the inclinometers moved outward. The readings obtained from SID-3, SIS-2, and SIS-4 showed insignificant displacements because they were all far from the location of the new piles.

PHASE III Excavation, Demolition, and New Foundation Slab:

The lateral displacements of the diaphragm wall at SID-1, SIS-4, and SID-3 after the completion of phase III construction are shown in Fig. 9(c). The displacement measurements were taken on 2014/12/30 with the initial readings set on 2014/5/26, prior to excavation, demolition, and construction of the new foundation slab. As shown in the figure, the diaphragm wall had a bulging deformation and the maximum wall displacements at SID-1, SIS-4, and SID-3 were 3 mm, 17 mm, and 20 mm, respectively.

The lateral displacement of the soil at SIS-1, SIS-2, and SIS-3 after the completion of phase III construction are shown in Fig. 10(c). The measurements were taken on exactly the same date as for those of SID-1, SIS-4, and SID-3. As shown in the figure, they also deformed with a bulging shape, with the exception of SIS-2, and the maximum wall displacements at SIS-1, SIS-2, and SIS-3 were 6 mm, 4 mm, and 7 mm, respectively.

The maximum displacement was 20 mm during the phase III construction, which is about 0.1% of the excavation depth. This displacement is smaller than 0.2% to 0.5% of the excavation depth, which is the maximum displacement induced by excavations (Ou 2006).

SID-4 and SID-5 were embedded in the newly constructed RC wall at the bottom of the foundation slab, *i.e.*, 18 m below the ground surface. The obtained displacements were negative, as shown in Fig. 11 because the bottom of the foundation slab was not a fixed point. The measured displacement at the top of the inclinometers was relative to the bottom of the foundation slab. When compared, the displacement behavior at SID-4 and SID-5 is similar to that at SIS-1 and SIS-3.

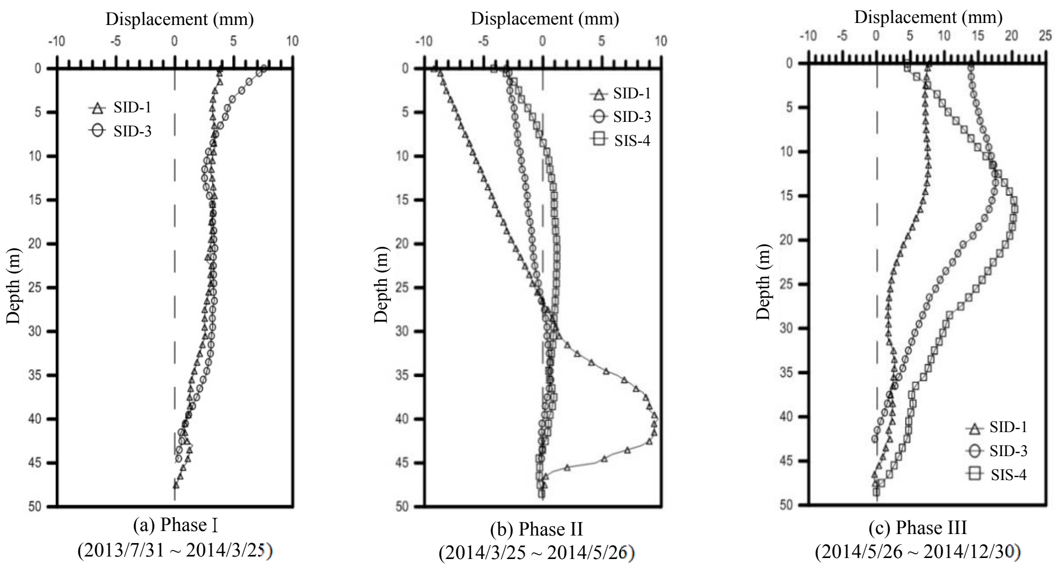

Fig. 9 Displacement increments in each Phase of the inclinometers SID-1, SID-3, SIS-4

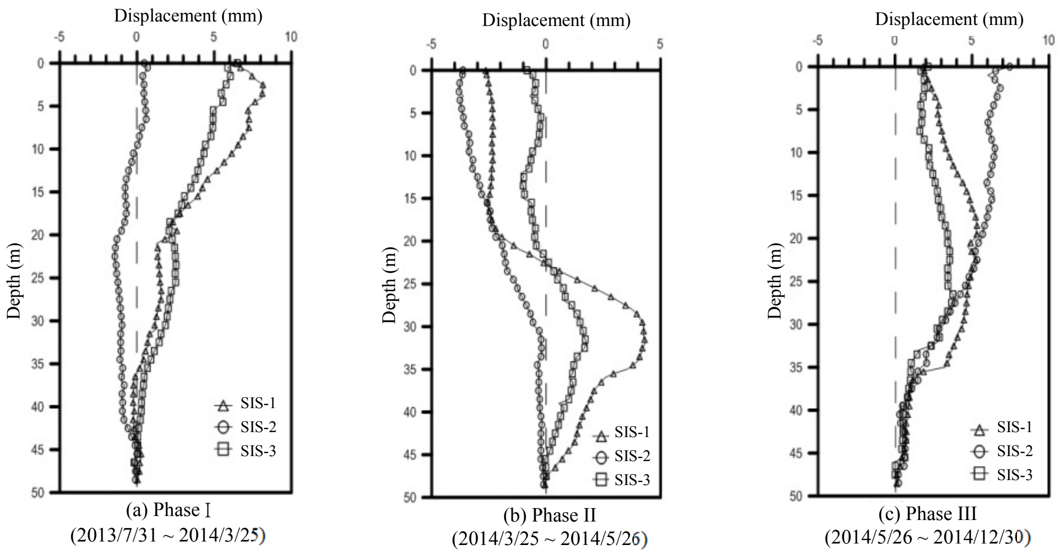

Fig. 10 Displacement increments in each Phase of the inclinometers SIS-1, SIS-2, SIS-3

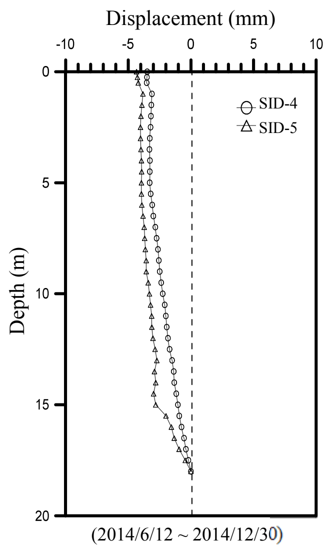

Fig. 11 Displacement increments at Phase III of the inclinometers SID-4, SID-5 for phase III

5.2 Stress of the Rebar

The rebar strain gauges at the location of RS-1 and RS-3 were damaged during construction and their data were not shown in this paper. As shown in Fig. 6, RS-2 was installed at the center of the new diaphragm wall and the stress conditions are representative of the behavior of the tube-like retaining wall. However, some vertical rebar strain gauges at RS-2 were damaged during construction, only 6 gauges remained functional during construction. Figure 12 shows the readings of the gauges in the vertical and horizontal rebar at the various depths at RS-2 where “a” indicates the gauges in the excavation side and “b” soil side. As shown in this figure, the horizontal rebar was subject to compressive force and the stress of the horizontal rebar was much higher than that of the vertical. The phenomenon was a typical of arch structures. This also confirms the arching effect of the tube-like retaining structure.

5.3 Ground Surface Settlement

The ground surface settlement at the end of construction for all settlement gauges is shown in Fig. 13(a). The ground surface settlement in the back of the new arch diaphragm wall is shown in Fig. 13(b). A concave type of the ground settlement was found where the maximum ground settlement was 7 mm occurring at a distance of 7 m behind the new arch diaphragm wall. In spite of the 7 mm ground surface settlement, which corresponds to 35% of the maximum displacement of 20 mm on the new arch diaphragm wall, this is considered an insignificant displacement as compared to the displacements obtained in the common excavations and construction practices in Taipei (Ou 2006).

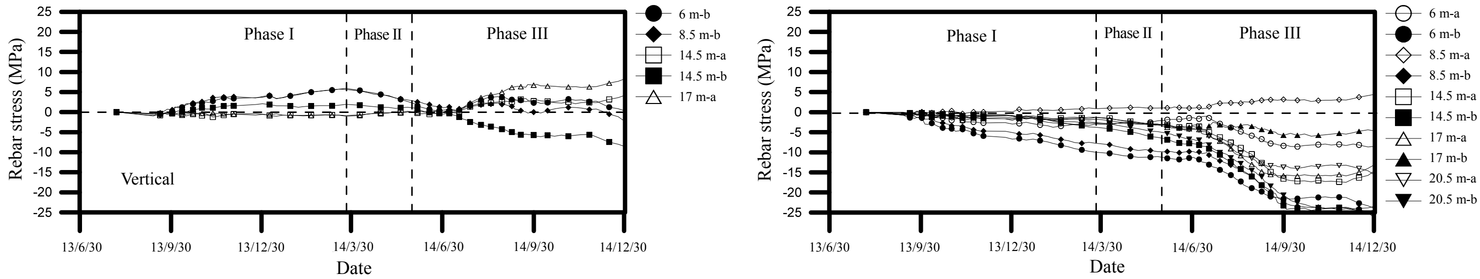

Fig. 12 RS-2 vertical and horizontal rebar stress of diaphragm wall ("a" indicate excavation side, "b" indicate soil side)

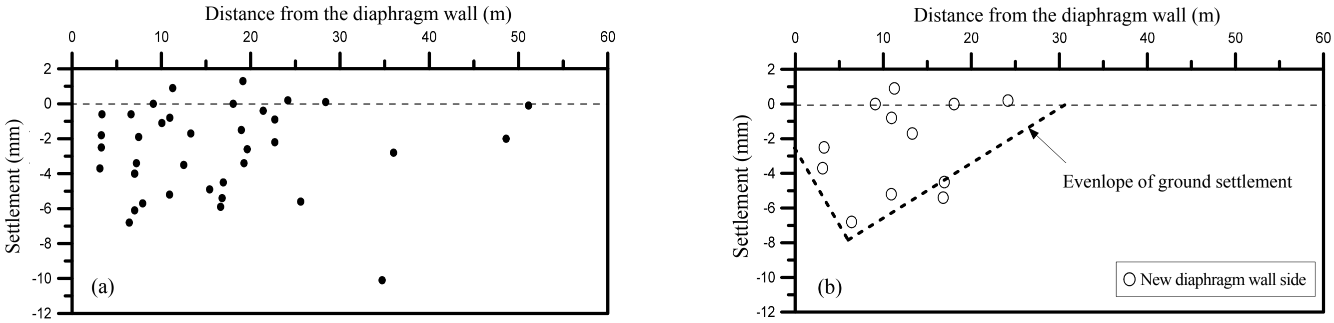

Fig. 13 Ground settlement of different distance (a) from diaphragm wall; (b) from new diaphgrgm wall

6. CONCLUSIONS

An old substructure was used as part of the retaining wall, followed by a strut-free excavation and demolition of the remaining basement. By examining the monitoring results, the following findings are concluded:

1. It is inevitable that one will encounter old underground structures in a building renovation project. By reinforcing the old underground structure and connecting it with a new diaphragm wall to form a tube-like underground structure, a new basement/foundation can be successfully completed without using any struts. Applying the arching effect developed by the tube-like structure not only reduces the construction duration but also ensures the construction's quality and safety.
2. The rebar strain gauges installed in the new arc retaining wall showed that the stress in the horizontal direction was higher than that in the vertical direction, which indicates that the tube-like retaining structure functions well.
3. The adoption of the tube-like retaining structure with a strut-free system results in a relatively smaller lateral displacement of wall and soil, and a smaller ground settlement compared with those observed in the common excavations in Taipei.
4. A pile foundation was applied in this project. Pile drilling also induced the lateral displacement of soil. In addition, according to the field monitoring results, the soil beneath the old foundation slab was disturbed due to the pile drilling and resulted in lateral displacements of soil. This occurred because the soil beneath the old foundation slab moved inward of the excavation area. As result of this inward movement of the earth layer toward the excavated area, the upper part of the new arch diaphragm wall had an outward movement.

REFERENCES

Lee, C.C. (2005). "The Da-Kang-Pu station of Kaohsiung mass rapid transit system — Design and construction of 140 m diameters circular diaphragm wall." *Sino-Geotechnics*, **105**, 5−16.

Ou, C.Y. (2006). *Deep Excavation—Theory and Practice*, Taylor and Francis.

Ou, C.Y., Chiou, D.C., and Wu, T.S. (1996). "Three-dimensional finite element analysis of deep excavation." *Journal of Geotechnical Engineering*, ASCE, **5**, 337−345.

Suroor, H., Galagoda, M., and McGhee, C. (2008). "Design and construction of circular secant pile walls in soft clays." *6th International Conference on Case Histories in Geotechnical Engineering*, Virginia, United States.

Tan, Y. and Wang, D. (2013). "Characteristics of a large-scale deep foundation pit excavated by the central-island technique in Shanghai soft clay. I: Bottom-up construction of the central cylindrical shaft." *Journal of Geotechnical and Geoenvironmental Engineering*, ASCE, **139**(11), 1875−1893.

Woo, S.M. and Moh, Z.C. (1990). "Geotechnical characteristics of soils in Taipei Basin." *Proceedings of the 10th Southeast Asian Geotechnical Conference*, Taipei, Taiwan, 51−65.